Energy barriers for Pb adatom diffusion on stepped ultrathin Pb(111) quantum nanofilms: First-principles calculations

Yong Han, James W. Evans, and Feng Liu

Phys. Rev. B **100**, 195405 — Published 5 November 2019

DOI: 10.1103/PhysRevB.100.195405

Energy barriers for Pb adatom diffusion on stepped ultrathin Pb(111) quantum nanofilms: first-principles calculations

Yong Han,[1,2,*] James W. Evans,[1,2] and Feng Liu[3]

[1] *Department of Physics and Astronomy, Iowa State University, Ames, Iowa 50011, USA*
[2] *Ames Laboratory, U. S. Department of Energy, Iowa State University, Ames, Iowa 50011, USA*
[3] *Department of Materials Science and Engineering, University of Utah, Salt Lake City, Utah 84112, USA*

Various properties of Pb(111) nanofilms, prototypical quantum films, have been studied extensively. However, key *ab-initio*-level energy barriers for Pb adatom diffusion on stepped Pb(111) nanofilm surfaces are still not available. Using first-principles density functional theory, we calculate these barriers for films with thicknesses of few monolayers (ML). We find that two-atom exchange is always much more favorable than direct hopping to cross A- or B-type steps. Ehrlich-Schwoebel (ES) barriers for downward transport to a higher-coordination step-edge site depend strongly on the film thickness. For such transport from 2- to 1-ML terraces, or from 4- to 3-ML terraces, there is no an ES barrier, but large ES barriers of more than 100 meV are found from 3- to 2-ML terraces. We also obtain the barriers for diffusion along the step edges and find that these step-edge barriers are significantly larger than terrace diffusion barriers. In addition, we analyze energetics for diffusion on the top flat surface of a nanofilm supported on a vicinal surface, and thus having underlying buried or ghost steps. We quantify the tilted potential energy surface in both ghost A- and B-step regions separating 2- and 3-ML (as well as 3- and 4-ML) terraces. Consequences are discussed for the growth kinetics of supported Pb nanofilms, where the support does not strongly effect electronic states within the film.

I. INTRODUCTION

Energy barriers related to adatom diffusion *across* steps on vicinal surfaces and more general multilayer surfaces control the transport of atoms over step edge. Consequently, these kinetic parameters guide the evolution of the growth morphology during physical vapor deposition. Specifically, they impact step meandering and bunching instabilities during step flow on vicinal surfaces, and also kinetic roughening associated with mounding instabilities during multilayer growth[1,2]. Energy barriers for diffusion *along* step edges control step meandering, the growth shapes of individual 2D islands nucleated on terraces, as well as post-deposition evolution of nonequilibrium 2D island shapes, e.g., during sintering[1–4].

Studies have traditionally considered thick films, where all terraces have the same adsorption energy and the same diffusion barrier. Then, the key single parameter impacting interlayer transport is the Ehrlich-Schwoebel (ES) barrier[5,6] which is defined as the additional energy barrier that must be overcome for downward transport at a step edge relative to the terrace diffusion barrier. (The ES barrier is set to be zero if there is no such excess energy.) The presence of such an additional barrier is generally regarded as being due to such fact that adatoms hopping across step edges have a lower number of neighbors in the transition state (TS) than for hopping on a terrace. We shall highlight below, however, the feature that exchange as well as hopping pathways are available for interlayer transport.

In this study, we will consider exclusively ultrathin Pb(111) nanofilms with the film thickness L up to several single-atom layers [or monolayers (ML)]. Our analysis will be for unsupported Pb nanofilms. However, these might be regarded as corresponding to nanofilms supported on a substrate which does not significantly impact the properties of electrons confined within the film. These films can exhibit the robust and regular oscillations in thermodynamic stability with increasing L, as observed in scanning tunneling microscopy (STM) experiments[7–10]. Such oscillations have been attributed to the quantum size effects (QSEs) originated from confinement of free electrons between two boundaries of the potential at two surfaces of a metal film[11]. QSEs reflect a matching relationship $2d \approx 3\lambda_F/2$ between the Fermi wavelength $\lambda_F = 0.396$ nm and the interlayer spacing $d = 0.284$ nm for Pb(111) film[12–15]. Previous first-principles density-functional-theory (DFT) calculations[14,16–18] reveal that the surface energy of Pb(111) films, as well as adatom adsorption energy and diffusion barrier on flat Pb(111) surfaces, exhibit oscillations as a function of L often with bilayer character. Therefore, for a stepped ultrathin Pb(111) film that we consider in the current contribution, the adsorption energies and diffusion barriers have distinct values on terraces (or regions) corresponding to different L, as will be described below. For such systems, there are different scenarios for the ES barrier, naturally defined as the additional energy barrier for downward transport relative to the diffusion on the upper terrace.

There are two distinct cases, illustrated in Figs. 1(a) and 1(b), where an adatom diffuses across a step between upper and lower terraces (and where the step edge site shown in the inset of Fig. 1 is most stable). Here, as is expected for metals, we assume no intralayer attachment barrier to the ascending step. For the case in Fig. 1(a) where the TS energy for diffusion on the upper terrace is higher than on the lower terrace, there are two quali-

TABLE I. Normal step-edge and ghost-step barriers (in meV) corresponding to Figs. 4 and 6. The first column lists the terrace thicknesses L, and an arrow indicates the diffusion direction from thickness L to $L-1$ or $L+1$. The second column is the note for normal step-edge or ghost-step, direct-hopping (hop) or two-atom-exchange (exc), and local or ES barriers. $A_\perp$ ($B_\perp$) stands for "across A (B) step", and $A_\parallel$ ($B_\parallel$) stands for "along A (B) step".

		$B_\perp$	$A_\perp$	$B_\parallel$	$A_\parallel$
$2 \to 1$	normal, hop, local	328	744	319	377
	normal, hop, ES	141	309		
	normal, exc, local	76	283		
	normal, exc, ES	0	0		
$3 \to 2$	normal, hop, local	470	483	242	464
	normal, hop, ES	417	441		
	normal, exc, local	210	158		
	normal, exc, ES	157	116		
$4 \to 3$	normal, hop, local	220	501	131	295
	normal, hop, ES	145	356		
	normal, exc, local	71	9		
	normal, exc, ES	0	0		
$2 \to 3$	ghost, hop, local	221	187		
$4 \to 3$	ghost, hop, local	118	89		

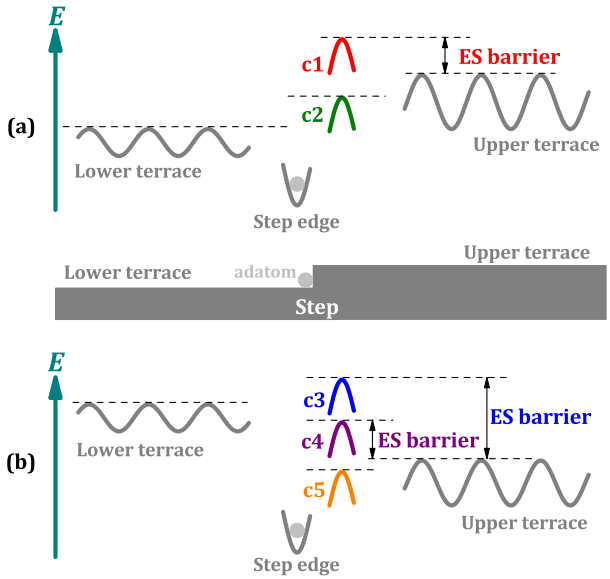

FIG. 1. Schematics of the possible potential-energy-surface forms for step crossing of an adatom when the TS energy for diffusion on the upper terrace is (a) above and (b) below the TS energy on the lower terrace. The deep well for the adatom at the step edge and different scenarios (c1, c2, c3, c4, and c5 with different colors) for the ES barrier are indicated. The inset in the middle illustrates the stepped surface with upper and lower terraces.

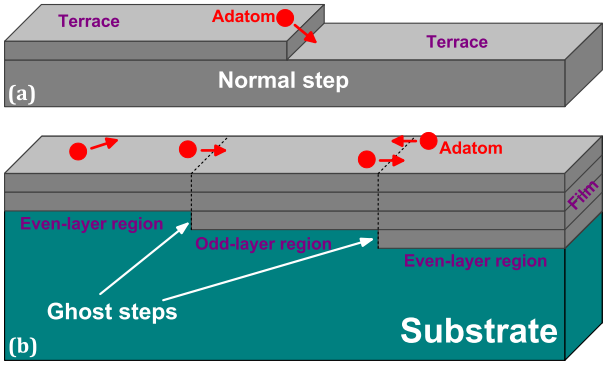

FIG. 2. Schematic illustration of adatom diffusion on (a) a surface with a normal step, and (b) a flat-top surface with the "ghost" steps buried at the bottom of the film supported on the stepped surface of a substrate.

tatively distinct scenarios c1 and c2. For c1 (red curve), the TS energy for step crossing is higher than the TS energy on the upper terrace, and therefore there is an ES barrier. For c2 (green curve), the TS energy for step crossing is lower than the TS energy on the upper terrace, and therefore there is no ES barrier. For the case in Fig. 1(b) where the TS energy for diffusion on the upper terrace is lower than on the lower terrace, there are three distinct scenarios c3, c4, and c5. For c3 (blue curve) or c4 (purple curve), the TS energy for step crossing is higher than the TS energy on the upper terrace, and therefore there is an ES barrier. For c5 (orange curve), the TS energy for step crossing is lower than the TS energy on the upper terrace, and therefore there is no ES barrier. For any scenario with an ES barrier (i.e., c1, c3, or c4), downward transport from the upper terrace is inhibited. For a scenario in which the TS energy for step crossing is above the TS energies on *both* upper and lower terraces (i.e., c1 or c3, but not c4), the presence of an ES barrier will impact transport between terraces, specifically it will reduce step permeability or transparency[19].

For ultrathin Pb(111) quantum nanofilms with steps on the surface, where adatoms can cross steps between thicker and thinner regions with thickness $L+1$ and L, DFT analysis of minimum energy paths (MEPs) and corresponding step-edge barriers has still not yet reported, although these barriers have been used as adjustable energetic parameters to analyze the kinetics and morphologies during the formation of Pb nanostructures on stepped Pb(111) nanofilms[20–23].

In experiments probing how the physical or chemical properties of specific atoms or molecules adsorbed on a Pb(111) film depend on film thickness, analysis for a film morphology different from conventional vicinal surface or multilayer film has proved particularly instructive. In these studies, a flat-top Pb nanofilm is first grown on a stepped substrate, e.g., on a Si(111) substrate with staircase-like steps[24–26]. Then, the flat-top Pb(111) film possesses a stepped bottom surface in order to match the substrate steps. Consequently, film thickness alternates between odd and even number of ML across these staircase-like steps, as illustrated in Fig. 2. For con-

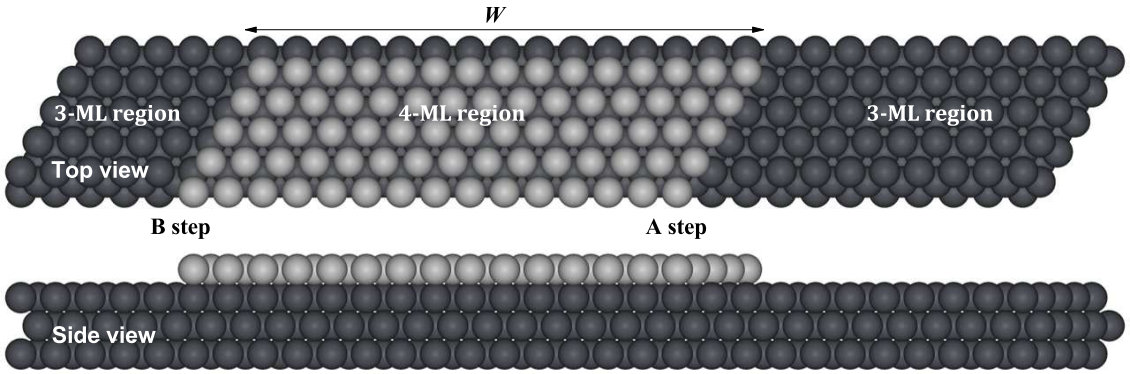

FIG. 3. Top and side views of the 30×5 supercell used to calculate Pb adatom diffusion on a stepped Pb(111) film surface with the A and B steps.

venience, we describe such buried or hidden steps as "ghost" steps. For contrast, we compare schematically a conventional stepped surface in Fig. 2(a) with a flat-top film including the ghost steps in Fig. 2(b). For the latter flat-top ultrathin Pb(111) nanofilms with the thicknesses of a few ML, the potential energy surface experienced by an adatom above a ghost step is different from those on other regions far from the ghost step. It is then natural to characterize the corresponding MEPs for adatom diffusion between regions of odd- and even-ML thicknesses. One can assess whether or not there exists an additional ES type barrier to cross ghost-step regions, as suggested previously[26]. In fact, the nucleation and growth behavior during the Pb deposition (e.g., island densities and island shapes) in the regions at and far from a ghost step are noticeably different, as shown by the STM image in Fig. 2 of Ref. 26. To analyze such behavior, knowledge of the MEP across the ghost step is valuable.

In this work, we perform the extensive first-principles DFT calculations for a Pb adatom diffusing on stepped ultrathin Pb(111) nanofilms with both normal and ghost steps within the thickness range from 1 to 4 ML. In experiments, a Pb film is generally supported on a substrate, but the inclusion of the substrate in the DFT calculations is a challenge because: (i) atomistic-level structure of the metal-substrate interface is often unknown, e.g., structure of the Pb-Si interface of relevance for this study still remains unclear; and (ii) computations can become very demanding upon inclusion of a substrate. Therefore, as noted above, the present calculations only consider the unsupported Pb films, i.e., we do not consider the contribution from substrate effects.

II. METHODOLOGY

Our DFT calculations are performed using the plane-wave-based Vienna *ab initio* simulation package (VASP) code[27]. We use the Perdew-Burke-Ernzerhof form of the generalized gradient approximation for the electronic exchange-correlation energy functional[28]. The electron-ion interactions are described by the projector augmented-wave approach[29]. The energy cutoff is taken to be the VASP default value 97.973 eV. Increasing the energy cutoff above this value do not significantly alter energy differences determining quantities of interest in our calculations. To prevent spurious interactions between adjacent replicas of the thin film system, we use a vacuum layer with the thickness not less than 1.5 nm in the direction perpendicular to the surface. The converged magnitude of the forces on all relaxed atoms is always less than 0.1 eV/nm. The optimized bulk lattice constant for fcc Pb is $a = 0.5035$ nm, as obtained previously[14]. All atoms are allowed to relax except those in the bottommost ML for vicinal surface are frozen with the fcc bulk lattice. For the ghost-step calculations, we fix the two bottommost ML. Minimum energy paths (MEPs) and corresponding energy barriers for Pb adatom diffusion on film surface are always determined via the climbing nudged-elastic-band (CNEB) method[30,31].

Before analyzing energetics for stepped films, we first perform benchmark calculations for a Pb adatom diffusing between fcc and hcp sites on the surface of a flat Pb(111) film with no steps (see Fig. S1[32] in Supplementary Material[32]) for a comparison with previous DFT results[18]. We select a 5×5 lateral unit cell (in units of surface lattice constant $a_0 = a/\sqrt{2}$) with a $\mathbf{k}$ mesh of $6 \times 6 \times 1$. Very similar MEP curves are obtained to those from more demanding DFT calculations[18], relative to which the errors in adsorption energies and diffusion barriers for 1- to 4-ML films are less than 10%. Thus, the accuracy for the parameter choice described above is sufficient for our focus in this work.

The adsorption energy E for a Pb adatom is always calculated as $E = E_{\rm tot} - E_{\rm cln} - E_{\rm Pb}$, where $E_{\rm tot}$ is the total energy of the film (modeled as a slab) with the adatom, $E_{\rm cln}$ is the total energy of a clean slab without adatom, and $E_{\rm Pb}$ is the self-energy of one gas-phase Pb atom. $E_{\rm tot}$, $E_{\rm cln}$, and $E_{\rm Pb}$ are directly obtained from DFT calculations. Note that the magnitude of the ad-

sorption energy at hcp site is always lower than that at fcc site for 2- to 4-ML films, and the transition state (TS) corresponding to a saddle point is *not* at the bridge site (for details, see Ref. 18 as well as Fig. S1[32]). The adsorption energy is oscillatory as a function of film thickness L due to QSEs, as mentioned in Sec. I and previously analyzed in detail in Ref. 18.

III. DIFFUSION ON NORMAL STEPPED SURFACES

A. Energetics

To analyze transport on a stepped film surface, we consider adatom diffusion across a 1-ML strip supported on slabs of various thicknesses using a lateral supercell size of 30×5. The two edges of the strip correspond to a {100}-microfaceted step (denoted as an A step) and a {111}-microfaceted step (a B step). If a_0 is the surface lattice constant, then the width of the strip is taken to be $W = 15a_0$, which is sufficiently large to avoid step-step interactions between adjacent replicas from our tests. The **k** mesh is taken to be $1 \times 6 \times 1$ for this supercell size. In Fig. 3, we show an example of the supercell for a 1-ML strip with two steps on a 3-ML film, where the 3- and 4-ML regions are marked.

We analyze behavior for the three thinnest slab thicknesses of 1, 2, and 3 ML, for which steps separate 1- and 2-ML terraces, 2- and 3-ML terraces, and 3- and 4-ML terraces, respectively. The MEPs of a Pb adatom diffusing across and along the A- and B-step edges are shown in Fig. 4. The local energy differences are also indicated in Fig. 4. All energy barriers for the diffusion processes across and along A and B steps are summarized in Table I. DFT adsorption energies of the adatom at hcp sites of 1-, 2-, 3-, and 4-ML regions (approximated as flat-slab surfaces without steps in Fig. S1[32]) as well as at the sites labeled in Fig. 4 are listed in Table S1[32]. Note that a hcp site is always more favorable than a fcc site for adsorption of an Pb adatom[18].

For the *1-ML-strip-on-1-ML-slab system* in Fig. 4(a), the local hopping barrier of 744 (328) meV across an A (B) step from site A1 to A2 to A3 (B1 to B2 to B3) is much larger than the two-atom exchange barrier of 283 (76) meV. Thus, two-atom exchange across either an A or B step is always more favorable than direct hopping. During the exchange, the adatom at site A2 (B1) pushes the A(B)-step-edge atom S, and then the atom S moves to site A4 (B3), simultaneously the adatom occupying the previous position of S [see Fig. 4(a)]. The ES barrier (as defined in Sec. I) of 309 (141) meV for hopping over an A (B) step is large, while there is no ES barrier for the two-atom exchange across A or B step, as listed in Table I. In addition, we also obtain the hopping barrier of 377 (319) meV for diffusion along the A(B)-step edge via the path of A3→A5→A4 (B3→B5→B4), as shown in Fig. 4(a) and listed in Table I. These barriers (377 and 317 meV) are more than three times of the barriers (around 100 meV) on 1- or 2-ML terrace.

For *1-ML-strip-on-2-ML-slab system* in Fig. 4(b), the local hopping barrier of 483 (470) meV across A (B) step from site A1 to Ab to A2 to A3 (B1 to Bb to B2 to B3) is three (two) times larger than the two-atom exchange barrier of 158 (210) meV, indicating that the two-atom exchange across either A or B step is always more favorable than direct hopping. During the exchange, the adatom at site Ab (Bb) pushes the A(B)-step-edge atom S, and then the atom S moves to site A4 (B3 or B4), simultaneously the adatom occupying the previous position of S [see Fig. 4(b)]. The ES barrier of 441 (417) meV for the hopping over A (B) step is large, relative to the smaller but still significant ES barrier of 116 (157) meV for the two-atom exchange across A (B) step, as listed in Table I. We also obtain the hopping barrier of 464 (242) meV for diffusion along the A(B)-step edge via the path of A3→A5→A4 (B3→B5→B4), as shown in Fig. 4(b) and listed in Table I.

For *1-ML-strip-on-3-ML-slab system* in Fig. 4(c), the local hopping barrier of 501 (220) meV across A (B) step from site A1 to Ab to A2 to A3 (B1 to B2 to B3) is much larger than the two-atom exchange barrier of 9 (71) meV, indicating that the two-atom exchange across either A or B step is always more favorable than direct hopping. During the exchange, the adatom at site Ab (B2) pushes the A(B)-step-edge atom S, and then the atom S moves to site A4 (B4), simultaneously the adatom occupying the previous position of S [see Fig. 4(c)]. The ES barrier of 356 (145) meV for the hopping over A (B) step is large, while there is no ES barrier for the two-atom exchange across A or B step, as listed in Table I. We also obtain the hopping barrier of 295 (131) meV for diffusion along A(B)-step edge via the path of A3→A5→A4 (B3→B5→B4), as shown in Fig. 4(c) and listed in Table I.

B. Kinetics

First, we discuss the consequences of our energetics results for *multilayer film growth* just in the few layer regime. Of particular relevance is the consequences for downward interlayer transport and for nucleation of islands on top of terraces. For a *1-ML island on a 1-ML film*, i.e., a 2-ML terrace surrounded by a 1-ML terrace [refer to Fig. 4(a)], there is a strong energetic preference for atoms deposited on top of the 1-ML island to attach at the island edge after downward transport. Given the absence of an ES barrier inhibiting downward transport, lateral growth of the 1-ML island is facilitated rather than nucleation of a new island on top of the 1-ML island (to create a 3-ML terrace). (The lack of an ES barrier is particularly significant for low-temperature versus high-temperature deposition.) Also, the adsorption energy is stronger on the lower 1-ML terrace versus on the 2-ML terrace, and there is additional binding at the step

edge. In addition, a 2-ML film has much lower surface energy than 1- and 3-ML films[18]. Thus, the expansion of a 1-ML island on a 1-ML film has a strong thermodynamic driving force versus the formation of a 3-ML film. The resulting 2-ML film is stable relative to 1- and 3-ML films, as observed in low-temperature (100 K) deposition experiments[33], where the Pb(111) films growing on highly-ordered pyrolytic graphite substrate are quasi-freestanding due to the very weak interaction between a Pb film and the graphite substrate.

In contrast, for a *1-ML island on a 2-ML film*, i.e., a 3-ML terrace surrounded by a 2-ML terrace [refer to Fig. 4(b)], it is much more likely for atoms deposited on top of the 1-ML island to nucleate a new island thereby creating a 4-ML terrace. At an A- or B-step edge, there is now a large ES barrier which inhibits the downward transport of atoms from the top of the 3-ML island, so nucleation and growth of a 1-ML island on the 3-ML terrace is kinetically preferred. Also, the adsorption energy is now weaker on the lower 2-ML terrace than on the 3-ML terrace, although binding at the A-step edge on the 2-ML terrace is slightly stronger. In addition, a 3-ML film has much higher surface energy than 2- and 4-ML films[18]. Therefore, the 3-ML island is unstable and a "bilayer" growth (i.e., from 2 to 4 ML) should appear during deposition, as already observed in the experiments for quasi-freestanding Pb(111) film growth[33].

For a *1-ML island on a 3-ML film*, i.e., a 4-ML terrace surrounded by a 3-ML terrace [refer to Fig. 4(c)], the fate of atoms deposited on top of the 1-ML island is analogous to that for a 1-ML island on a 1-ML film. Downward transport and attachment to the edge of the 1-ML island to grow the 4-ML region is preferred thermodynamically, and aided kinetically by the absence of an ES barrier (including for low-temperature deposition). Indeed, stability of a 4-ML film against 3- and 5-ML films is observed in low-temperature deposition experiments for quasi-freestanding Pb(111) film growth[33]. We caution that the connection of our theoretical analysis to experimental observations for Pb film growth on a Si substrates[7–10] is complicated by the strong film-substrate interaction. This can result in a shift with respect to L of basic features of the energetic parameters relative to that for freestanding Pb(111) films[14,16–18]. However, we believe that qualitative features of the shift in behavior determined upon increasing thickness for unsupported films will be preserved for supported films.

It is appropriate to compare the results of our DFT analysis for ES barriers with previous modeling of experimental observations[21,22]. The latter included no ES barrier for downward transport from terraces with a weaker to stronger adsorption energy, consistent with our results. An ES barrier of 0.15 eV was included for downward transport from terraces with a stronger to a weaker adsorption energy. This should be compared to our results of 0.12 (0.16) eV for A (B) step between 3 ML and 2 ML terraces. We caution, however, that the previous modeling included various other assumptions about energetics in the Pb multilayer system.

Next, we briefly comment on behavior for *step flow on vicinal Pb(111) surfaces* drawing upon our energetics results. For low temperature or broad terraces, island formation occurs during deposition where the island density is controlled by the terrace diffusion barrier. However, for higher temperature or narrow terraces, most atoms reach step edges leading to step flow. The presence of a significant ES barrier between $(2L)$- and $(2L+1)$-ML terraces, but not between $(2L-1)$- and $(2L)$-ML terraces, implies that step flow should lead to step pairing. Specifically, the resulting film has significant population of even-ML [$(2L)$-ML] terraces (stable) and a negligible population of odd-ML [$(2L-1)$- and $(2L+1)$-ML] terraces (unstable). Fig. 5 indicates which steps capture adatoms deposited at various locations, and thus demonstrates the faster propagation of steps between $(2L-1)$- and $(2L)$-ML terraces than between $(2L)$- and $(2L+1)$-ML terraces.

IV. DIFFUSION IN THE PRESENCE OF GHOST STEPS

A. Energetics

To analyze transport in the presence of ghost steps, one can consider adatom diffusion across a flat L-ML slab with an underlying 1-ML strip bounded by both A and B steps. We analyze such systems for only $L = 2$ and 3 in this work. For $L = 3$, the analysis corresponds to adatom diffusion across the bottom surface of the configuration shown in Fig. 3. In calculations for these systems with ghost steps, we take the lateral supercell size to be 10×5 with the $\mathbf{k}$ mesh of $3 \times 6 \times 1$ and the width of the 1-ML strip to be $W = 5a_0$. These parameter settings are rougher than those used in calculations for the systems with normal steps in Sec. III, but from our tests[18] they are still sufficiently accurate for our purpose in this work.

As described in the previous sections, because of QSEs, there is a large adsorption energy difference between 2- and 3-ML (or 3- and 4-ML) regions for a 2-ML (or 3-ML) slab. However, for adatom diffusion on the top flat surface of a slab with underlying ghost steps, there are no deep wells corresponding to higher-coordination adsorption sites like those at a normal step edge. Thus, the oscillatory potential energy surface or MEP in a ghost-step region between two regions with thickness L and $L+1$ will vary more regularly. In the zeroth-order picture, the MEP in a ghost-step region can be regarded as a version distorted by a steep gradient relative to the periodic MEP on a flat surface without any steps. This behavior is revealed in Fig. 6.

Another feature is that, in a ghost-step region, there are strongly varying local hopping barriers along a path across a ghost step despite the feature that diffusion occurs on a flat surface of the slab. There always exists a relatively large local barrier encountered in traversing a ghost-step region. Such relatively large local barriers for

A and B ghost steps are labeled by P and Q in Fig. 6. These local ghost-step barriers are summarized in Table I. DFT adsorption energies of the adatom at hcp sites of 2-, 3-, and 4-ML regions (approximated as flat-slab surfaces without steps in Fig. S1[32]) as well as at the sites labeled in Fig. 6 are listed in Table S2[32]. Here we need to state that, for the systems in Fig. 6, although the local barriers at P or Q is large, there is no an ES-type barrier because the energies at P or Q are always lower than the TS energy on the 2- or 4-ML region, and thus these barriers do not globally impact the mass transport from the 2- or 4-ML region to the 3-ML region.

B. Kinetics

First, we consider diffusion on a flat slab with alternating 2- and 3-ML regions corresponding to Fig. 6(a). For low enough temperature where transport between terraces is limited and island formation is irreversible, the island density in the 3-ML region will be significantly lower than in the 2-ML region noting that the diffusion barrier of 39 meV on 3-ML region is much less than 102 meV on 2-ML region. The situation is more complicated for reversible island formation. For higher temperature where atoms deposited on the 2-ML region can reach the 3-ML region before nucleating terraces, they will accumulate on the 3-ML region given the significantly stronger adsorption (by 494 meV). A similar discussion applies for a flat slab with alternating 3- and 4-ML regions corresponding to Fig. 6(b). Here the adsorption energy difference is 167 meV, and the diffusion barrier of 39 meV on 3-ML region is less than 55 meV on 4-ML region.

For a flat Pb(111) film supported on a vicinal substrate which presents an extended sequence of ghost steps, the alternating sequence of even- and odd-ML regions will produce an alternating sequence of regions with higher and lower adsorption energy, at least, if the regions are not too thick[24–26]. This type of situation has been considered in the context of directed assembly on templated substrates[34]. In general, it is not just stronger adsorption which directs nucleation, but lower diffusion barriers, since the latter enhances the nucleation rate.

V. CONCLUSIONS

In conclusion, we have performed the first-principles DFT calculations to obtain energy barriers of a Pb adatom diffusing on stepped ultrathin Pb(111) film surfaces. To cross an A- or B-type step, the two-atom exchange is always much more favorable than direct hopping, and the ES barrier strongly depends on the film thickness. For steps between 2- and 1-ML terraces, or between 4- and 3-ML terraces, there is no an ES barrier. For steps between 3- and 2-ML terraces, large ES barriers of more than 100 meV are found. Along the step edges, the barriers are found to be significantly larger than those for terrace diffusion on a flat surfaces without steps. Barriers for interlayer transport are shown to strongly impact morphological evolution during deposition either for multilayer growth or for step flow. We also analyze diffusion on flat surfaces with underlying ghost steps where difference in adsorption energies and diffusion barriers for regions of different thicknesses can lead to directed-assembly via nucleation and growth of Pb islands during deposition.

ACKNOWLEDGMENTS

Y.H. and J.W.E. were supported for this work by NSF Grant No. CHE-1507223, and their work was performed at Ames Laboratory which is operated for the U. S. Department of Energy (USDOE) by Iowa State University under Contract No. DE-AC02-07CH11358. Our computations utilized the resources from the NSF-supported Extreme Science and Engineering Discovery Environment (XSEDE) served by Texas Advanced Computing Center (TACC), the USDOE-supported National Energy Research Scientific Computing Center (NERSC), and the Center for High Performance Computing (CHPC) at University of Utah.

* Electronic mail: y27h@ameslab.gov

[1] T. Michely and J. Krug, *Islands, Mounds, and Atoms* (Springer, Berlin, 2004).
[2] J. W. Evans, P. A. Thiel, and M. C. Bartelt, Surf. Sci. Rep. **61**, 1 (2006).
[3] M. Einax, W. Dieterich, and P. Maass, Rev. Mod. Phys. **85**, 921 (2013).
[4] K. C. Lai, Y. Han, P. Spurgeon, W. Huang, P. A. Thiel, D.-J. Liu, and J. W. Evans, Chem. Rev. **119**, 6670 (2019).
[5] G. Ehrlich and F. G. Hudda, J. Chem. Phys. **44**, 1039 (1966).
[6] R. L. Schwoebel and E. J. Shipsey, J. Appl. Phys. **37**, 3682 (1966).
[7] H. Hong, C.-M. Wei, M. Y. Chou, Z. Wu, L. Basile, H. Chen, M. Holt, and T.-C. Chiang, Phys. Rev. Lett. **90**, 076104 (2003).
[8] M. H. Upton, C. M. Wei, M. Y. Chou, T. Miller, and T.-C. Chiang, Phys. Rev. Lett. **93**, 026802 (2004).
[9] P. Czoschke, H. Hong, L. Basile, and T.-C. Chiang, Phys. Rev. Lett. **93**, 036103 (2004).
[10] Y.-F. Zhang, J.-F. Jia, T.-Z. Han, Z. Tang, Q.-T. Shen, Y. Guo, Z. Q. Qiu, and Q.-K. Xue, Phys. Rev. Lett. **95**, 096802 (2005).
[11] F. K. Schulte, Surf. Sci. **55**, 427 (1976).
[12] B. J. Hinch, C. Koziol, J. P. Toennies, and G. Zhang, Europhys. Lett. **10**, 341 (1989).

[13] T. Miller, M. Y. Chou, and T.-C. Chiang, Phys. Rev. Lett. **102**, 236803 (2009).
[14] Y. Han and D.-J. Liu, Phys. Rev. B **80**, 155404 (2009).
[15] R.-Y. Liu, A. Huang, C.-C. Huang, C.-Y. Lee, C.-H. Lin, C.-M. Cheng, K.-D. Tsuei, H.-T. Jeng, I. Matsuda, and S.-J. Tang, Phys. Rev. B **92**, 115415 (2015).
[16] C. M. Wei and M. Y. Chou, Phys. Rev. B **66**, 233408 (2002).
[17] T.-L. Chan, C. Z. Wang, M. Hupalo, M. C. Tringides, and K. M. Ho, Phys. Rev. Lett. **96**, 226102 (2006).
[18] W. Li, L. Huang, R. G. S. Pala, G.-H. Lu, F. Liu, J. W. Evans, and Y. Han, Phys. Rev. B **96**, 205409 (2017).
[19] R. Zhao, J. W. Evans, and T. J. Oliveira, Phys. Rev. B **93**, 165411 (2016).
[20] Z. Kuntova, M. Hupalo, Z. Chvoj, and M. Tringides, Surf. Sci. **600**, 4765 (2006).
[21] Z. Kuntova, M. Hupalo, Z. Chvoj, and M. C. Tringides, Phys. Rev. B **75**, 205436 (2007).
[22] Z. Kuntová, M. C. Tringides, and Z. Chvoj, Phys. Rev. B **78**, 155431 (2008).
[23] Z. Kuntová, M. C. Tringides, S. M. Binz, M. Hupalo, and Z. Chvoj, Surf. Sci. **604**, 519 (2010).
[24] L.-Y. Ma, L. Tang, Z.-L. Guan, K. He, K. An, X.-C. Ma, J.-F. Jia, Q.-K. Xue, Y. Han, S. Huang, and F. Liu, Phys. Rev. Lett. **97**, 266102 (2006).
[25] X. Ma, P. Jiang, Y. Qi, J. Jia, Y. Yang, W. Duan, W.-X. Li, X. Bao, S. B. Zhang, and Q.-K. Xue, Proc. Natl. Acad. Sci. U. S. A. **104**, 9204 (2007).
[26] S. M. Binz, M. Hupalo, and M. C. Tringides, Phys. Rev. B **78**, 193407 (2008).
[27] G. Kresse and J. Hafner, Phys. Rev. B **47**, 558 (1993).
[28] J. P. Perdew, K. Burke, and M. Ernzerhof, Phys. Rev. Lett. **77**, 3865 (1996).
[29] G. Kresse and D. Joubert, Phys. Rev. B **59**, 1758 (1999).
[30] G. Henkelman, B. P. Uberuaga, and H. Jónsson, J. Chem. Phys. **113**, 9901 (2000).
[31] G. Henkelman and H. Jónsson, J. Chem. Phys. **113**, 9978 (2000).
[32] See Supplemental Material at [URL will be inserted by the production group] for MEPs of Pb adatom hopping from hcp to fcc sites on flat Pb(111) film surfaces with thicknesses $L = 1$ to 4 ML (see, also, references 18 and 35 therein). Tables S1 and S2 provide the DFT adsorption energies in Figs. 4 and 6, respectively.
[33] J. H. Dil, T. U. Kampen, B. Hülsen, T. Seyller, and K. Horn, Phys. Rev. B **75**, 161401 (2007).
[34] X. Niu, R. Vardavas, R. E. Caflisch, and C. Ratsch, Phys. Rev. B **74**, 193403 (2006).
[35] G. Farin, *Curves and Surfaces for CAGD: A Practical Guide* (Academic Press, San Diego, 2002) 5th edition.

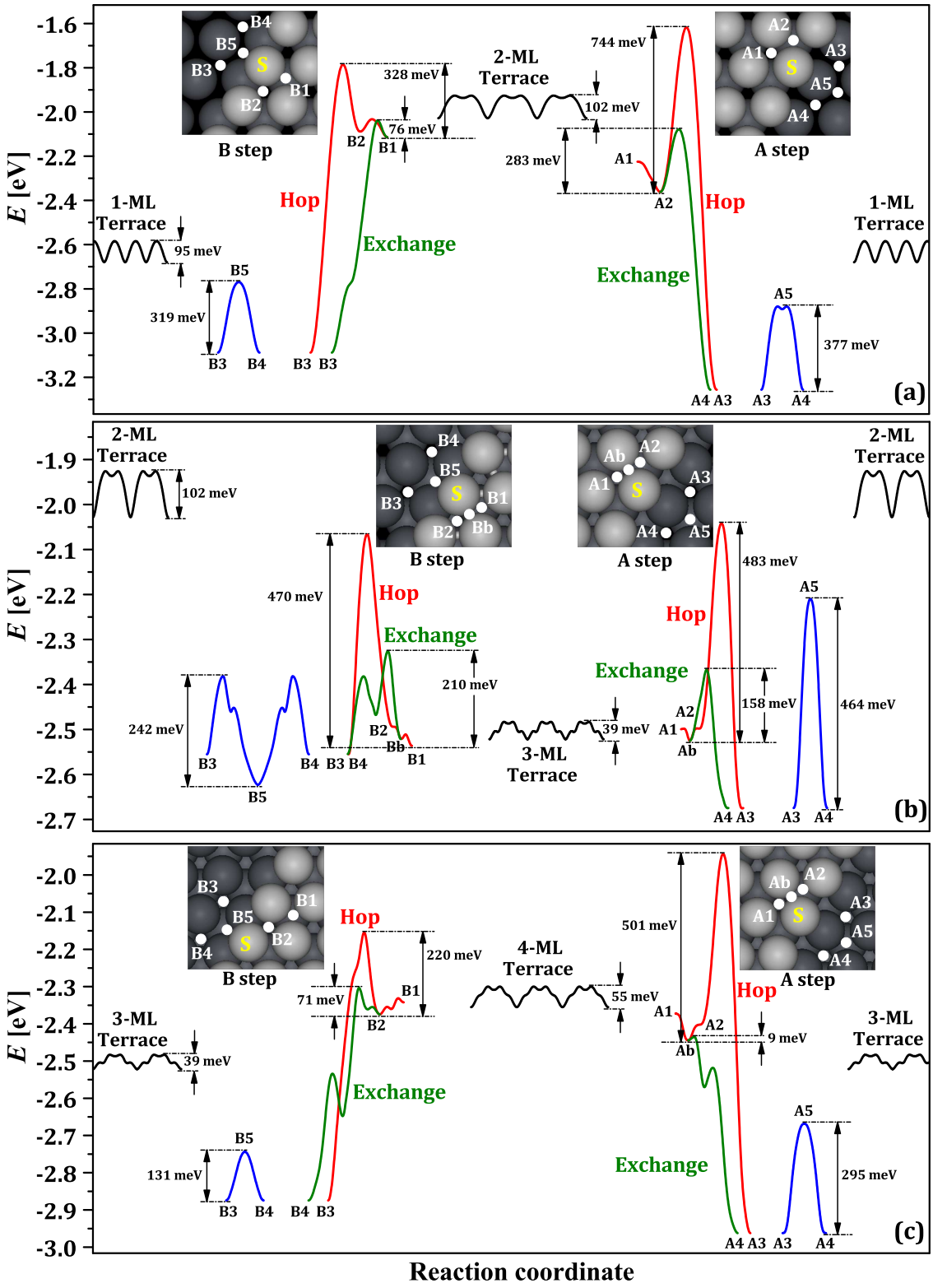

FIG. 4. MEPs calculated from the DFT plus CNEB method for a Pb adatom diffusing across A and B steps with a 1-ML strip (light color) on (a) 1-, (b) 2-, and (c) 3-ML Pb(111) films (dark color). Insets indicate the step geometries and local equilibrium sites (white dots with labels). For more details, see text.

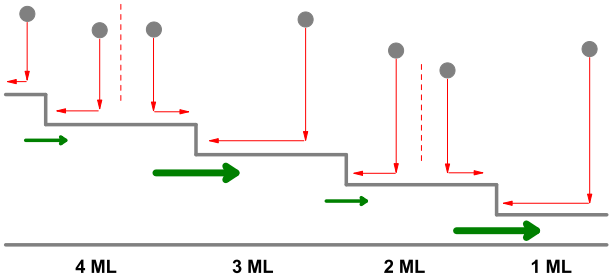

FIG. 5. Step pairing during deposition on a vicinal Pb(111) nanofilm. The schematic illustrates which steps capture atoms deposited at various locations, leading to assessment of step propagation velocities indicated by thick green arrows.

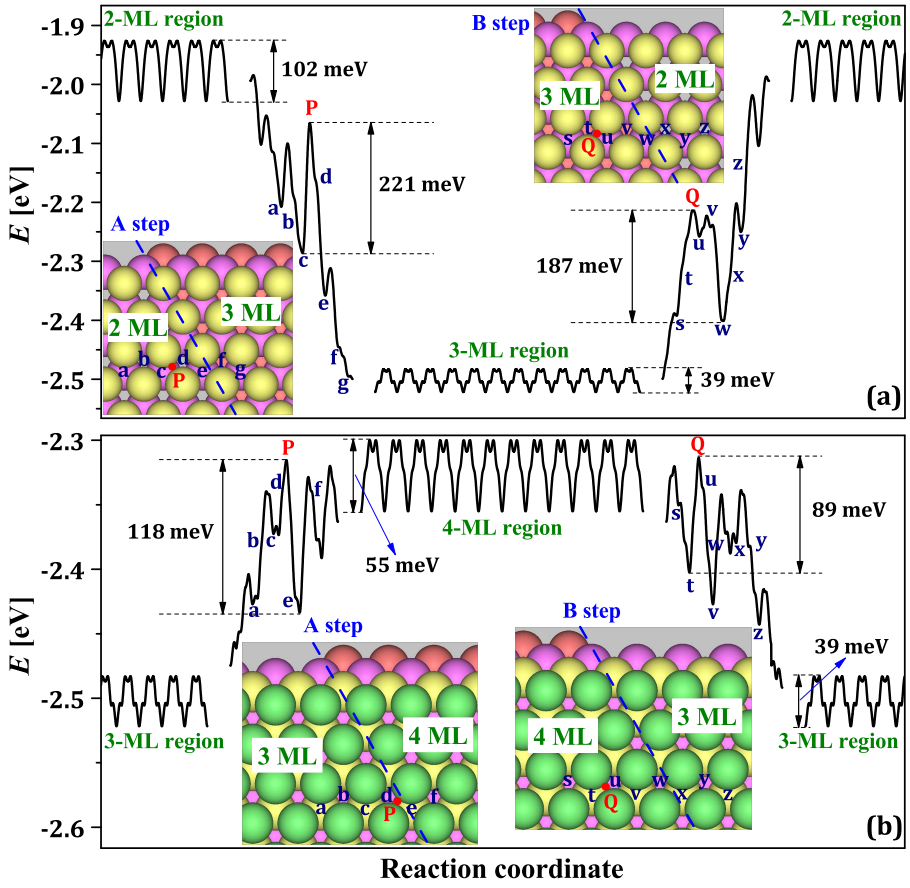

FIG. 6. MEPs calculated from the DFT plus CNEB method for a Pb adatom diffusing across A and B ghost steps with a 1-ML strip underneath (a) 2- and (b) 3-ML Pb(111) films. Colors are used to identify the different ML. Insets indicate the step geometries and local equilibrium sites (blue lowercase letters). P and Q indicate the ghost-step barriers. Dashed blue lines approximately mark the step positions. For more details, see text.